# *Improvement of the boron neutron capture therapy (BNCT) by the previous administration of the histone deacetylase inhibitor sodium butyrate for the treatment of thyroid carcinoma*

**M. Perona, C. Rodríguez, M. Carpano, L. Thomasz, S. Nievas, M. Olivera, S. Thorp, P. Curotto, E. Pozzi, S. Kahl, M. Pisarev, G. Juvenal, et al.**

**Radiation and Environmental Biophysics**

ISSN 0301-634X

Radiat Environ Biophys
DOI 10.1007/s00411-013-0470-0

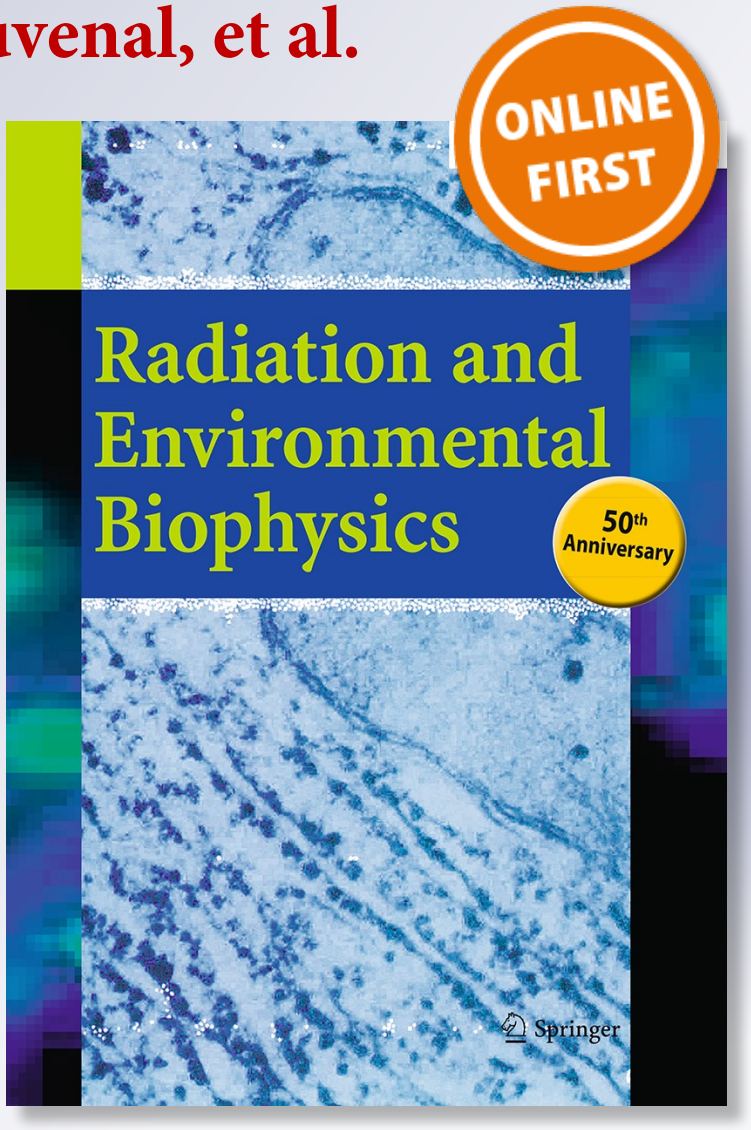


Springer

Radiat Environ Biophys
DOI 10.1007/s00411-013-0470-0

ORIGINAL PAPER

# Improvement of the boron neutron capture therapy (BNCT) by the previous administration of the histone deacetylase inhibitor sodium butyrate for the treatment of thyroid carcinoma

**M. Perona · C. Rodríguez · M. Carpano · L. Thomasz · S. Nievas · M. Olivera · S. Thorp · P. Curotto · E. Pozzi · S. Kahl · M. Pisarev · G. Juvenal · A. Dagrosa**

Received: 29 May 2012 / Accepted: 10 April 2013


**Abstract** We have shown that boron neutron capture therapy (BNCT) could be an alternative for the treatment of poorly differentiated thyroid carcinoma (PDTC). Histone deacetylase inhibitors (HDACI) like sodium butyrate (NaB) cause hyperacetylation of histone proteins and show capacity to increase the gamma irradiation effect. The purpose of these studies was to investigate the use of the NaB as a radiosensitizer of the BNCT for PDTC. Follicular thyroid carcinoma cells (WRO) and rat thyroid epithelial cells (FRTL-5) were incubated with 1 mM NaB and then treated with boronophenylalanine $^{10}$BPA (10 μg $^{10}$B ml$^{-1}$) + neutrons, or with 2, 4-*bis* (α,β-dihydroxyethyl)-deutero-porphyrin IX $^{10}$BOPP (10 μg$^{10}$B ml$^{-1}$) + neutrons, or with a neutron beam alone. The cells were irradiated in the thermal column facility of the RA-3 reactor (flux = (1.0 ± 0.1) × $10^{10}$ n cm$^{-2}$ s$^{-1}$). Cell survival decreased as a function of the physical absorbed dose in both cell lines. Moreover, the addition of NaB decreased cell survival ($p < 0.05$) in WRO cells incubated with both boron compounds. NaB increased the percentage of necrotic and apoptotic cells in both BNCT groups ($p < 0.05$). An accumulation of cells in G2/M phase at 24 h was observed for all the irradiated groups and the addition of NaB increased this percentage. Biodistribution studies of BPA (350 mg kg$^{-1}$ body weight) 24 h after NaB injection were performed. The in vivo studies showed that NaB treatment increases the amount of boron in the tumor at

A. Dagrosa and G. Juvenal should be considered as joint authors.

M. Perona · C. Rodríguez · M. Carpano · L. Thomasz · M. Pisarev · G. Juvenal (✉) · A. Dagrosa (✉)
Department of Radiobiology, National Atomic Energy Commission (CNEA), Avenida General Paz 1499, San Martín (1650), Buenos Aires, Argentina
e-mail: juvenal@cnea.gov.ar

A. Dagrosa
e-mail: mariaalejandradgrs3@gmail.com

L. Thomasz · M. Pisarev · G. Juvenal · A. Dagrosa
National Research Council of Argentina (CONICET), Avenida Rivadavia 1917 (1033), Ciudad Autónoma de Buenos Aires, Argentina

S. Nievas · M. Olivera
Department of Boron Neutron Capture Therapy, CNEA, Avenida General Paz 1499, San Martín (1650), Buenos Aires, Argentina

S. Thorp
Department of Instrumentation and Control, CNEA, Presbitero Juan Gonzalez y Aragón No 15 (1802), Ezeiza, Buenos Aires, Argentina

P. Curotto · E. Pozzi
RA-3 reactor, Research and Production Reactors, CNEA, Presbitero Juan Gonzalez y Aragón No 15 (1802), Ezeiza, Buenos Aires, Argentina

S. Kahl
Department of Pharmaceutical Chemistry, University of California, 6th Street UCSF Box 2280, Room GH-518, San Francisco, CA 94143, USA

M. Pisarev
Department of Human Biochemistry, School of Medicine, University of Buenos Aires, Paraguay 2155 (1121), Ciudad Autónoma de Buenos Aires, Argentina

Published online: 01 May 2013

2-h post-BPA injection ($p < 0.01$). We conclude that NaB could be used as a radiosensitizer for the treatment of thyroid carcinoma by BNCT.

**Keywords** Sodium butyrate · Radiosensitizer · Thyroid cancer · BNCT

## Introduction

Thyroid cancer is one of the most common endocrine tumors and represents about 0.5–1.5 % of all tumors. There are effective treatments for well-differentiated tumors, such as gland ablation, followed by the administration of $^{131}$I or suppression of thyroid-stimulating hormone (TSH) with thyroid hormone. However, there is a small proportion of patients with tumor recurrence that do not respond to any of the conventional therapies (Brierley and Tsang 2008).

Boron neutron capture therapy (BNCT) is a tumor-selective treatment modality. At present, clinical trials are being performed in several countries in the world, including Italy, Taiwan, Japan, Finland and Argentina, for those malignancies that do not respond to standard therapies (Kageji et al. 2011). BNCT is considered a method of radiation therapy based on the selective uptake of the boron compound by tumoral tissue in comparison with surrounding normal tissue. Once the concentration of boron is appropriated, the tumor is irradiated with a thermal neutron beam. $^{10}$B turns into $^{11}$B which immediately decays and releases an alpha particle and a $^{7}$Li nucleus. These particles of high-linear energy transfer (LET) are lethal for the boron-containing cells (Joensuu et al. 2011).

We have performed in vitro and in vivo studies in order to apply BNCT to undifferentiated and poorly differentiated thyroid cancer. We evaluated two boron compounds, boronophenylalanine (BPA) and tetrakis-carborane carboxylate ester of 2,4-*bis*-(*a*, *b*-dihydroxyethyl)-deuteroporphyrin IX (BOPP), alone and combined. These studies showed that the smaller tumors achieved a complete regression and the bigger ones only a stop in the growth for a short time (Dagrosa et al. 2007). Different strategies like the combination with other treatments could be effective to improve the outcome of BNCT.

Histone proteins organize DNA into nucleosomes, which are regular repeating structures of chromatin. The acetylation status of histones alters the chromatin structure, which, in turn, is involved in gene expression. Two classes of enzymes can affect the acetylation of histones: histone acetyltransferases (HATs) and histone deacetylases (HDACs). A number of HDAC inhibitors (HDACI) that inhibit tumor growth in vitro and in vivo at doses that have little or no toxicity have been characterized (Butler et al. 2001).

Sodium butyrate (NaB) is the sodium salt of butyric acid which is a normal fatty acid occurring in the form of esters in animal and plant oils. This compound is a HDACI involved in different epigenetically controlled activities like apoptosis, proliferation, cell differentiation, induction of cell cycle arrest and motility (Muhlethaler-Mottet et al. 2008). Moreover, it was described that HDACI increase the sensitivity to gamma radiation in different cell lines (Leith 1988; Munshi et al. 2005). Besides, it has a direct antitumoral activity by itself. Therefore, this compound presents two mechanisms of action, increased radiosensitivity and direct antiproliferative action. These make it a potential effective compound for the treatment of cancer (Xu et al. 2007).

In the present studies, we analyze the possibility of using the HDACI sodium butyrate as a radiosensitizer for BNCT in the treatment of thyroid cancer.

## Materials and methods

### Cell line

The human thyroid follicular cancer cell line WRO (kindly provided by Dr. Julliard, UCLA) and the Fisher rat thyroid (FRTL-5) cell line were grown and kept at 37 °C in 5 % $CO_2$–95 % air atmosphere in a humidified incubator. The WRO cell line was cultured in RPMI 1640 (GIBCO, Invitrogen Corporation, USA) medium with glutamine supplemented with 10 % fetal bovine serum (FBS) (Natocor, Córdoba, Argentina), whereas the FRTL-5 cell line was cultured in Dulbecco's modified Eagle medium (DMEM/F12, 50:50 v/v) (GIBCO) supplemented with 5 % FBS bovine, thyrotropin (1 mU ml$^{-1}$), hydrocortisone (3.62 ng ml$^{-1}$), transferrin (5 μg ml$^{-1}$), insulin (10 mg ml$^{-1}$), somatostatin (10 ng ml$^{-1}$) and glycyl-L-histidyl-L-lysine acetate (10 ng ml$^{-1}$) (Sigma, St Louis, MO, USA).

### Animal model

NIH nude mice (body weight 20–25 g) were implanted in the back right flank with $10^6$ cells of the human WRO cell line. The animals were bred and maintained under sterile conditions (US Department of Health and Human Services 1985). After 15 days, when the tumors had a size between 25 and 100 mm$^3$, the mice were used for the biodistribution studies of boron compounds.

### Preparation of boron solutions

The stock solution of boronophenylalanine $^{10}$BPA-fructose was prepared at a concentration of 30 mg $^{10}$BPA per ml

(0.14 M). $^{10}$BPA (99 % $^{10}$B enriched, L-isomer) (Glyconix Corp, Raleigh, NC, USA) was combined in water with a 10 % molar excess of fructose. The pH was then adjusted to 9.5–10 with NaOH, and the mixture was stirred until all solids dissolved. Afterward, the pH was readjusted to 7.4 with HCl.

The $^{10}$BOPP (tetrakis-carborane carboxylate ester of 2,4-*bis*-(*a*, *b*-dihydroxyethyl)-deutero-porphyrin IX) stock solutions (10 mg ml$^{-1}$) were prepared in phosphate-buffered saline (PBS 1X) and stored at 4 °C in darkness for no more than 24 h. The experiments with $^{10}$BOPP were performed under conditions of low intensity light, since solutions of porphyrins are known to be sensitive to visible light (Kahl and Koo 1992).

## Evaluation of NaB toxicity

To evaluate the effect of the drug on cell viability, 2,000 cells of both cell lines were seeded in 200 µl of the respective culture medium on 96-well plates. They were incubated for 24 and 48 h with increasing concentrations of sodium butyrate (NaB) (0; 0.3; 0.5; 0.8; 1; and 1.5 mM). Then, 20 µl of vital dye 3-(4,5 dimethylthiazol-2-yl)-2,5 diphenyltetrazoliumbromide (MTT) [Sigma 128] 0.5 % w/v in PBS was added to the culture medium and absorbance at 540 nm was read. Results are expressed as percentage of untreated controls.

## Western blot analysis

For Western blot analysis, WRO and FRTL-5 cells were incubated with 1 mM NaB for 24 h. Cells were washed twice in cold PBS, harvested and centrifuged. The PBS was removed and the pellet was lysed in 100 µl of RIPA buffer (50 mM Tris–HCl, pH 7.2, 150 mM NaCl, 1 % Nonidet P-40, 1 % sodium deoxycholate, 0.1 % SDS) containing protease inhibitors. The cell lysate was cleared by centrifugation and the supernatant was used as a total cellular protein extract. Protein concentration was determined by Bradford protein assay (BioRad). From each sample, 60 µg of total protein was loaded into a 12 % SDS-polyacrylamide gel and electrophoresed at 90 V for 2 h. The separated proteins were transferred to a *Hybond-P* membrane (Amersham) in transfer buffer (25 mM Tris base, 192 mM glycine, 20 % methanol, 0.05 % SDS) at 100 V during 1 h at 4 °C. The membrane was probed with goat antibody raised against acetyl-histone H3 (sc-8655, Ac-Histone H3 (lys 9/14), Santa Cruz CA, USA). Beta-actin monoclonal antibody (Clone AC-15, Sigma) was used as a loading control. The membrane was washed and incubated with the secondary antibody (anti-goat antibody conjugated to horseradish peroxidase, Vector Laboratories, CA, USA). The bands were visualized by chemiluminescence after the addition of substrate (ECL detection kit, Amersham) and exposed to autoradiograph films. Semiquantitative analysis was obtained after the films were scanned with a densitometer to determine the density of each band. The relative optical density (OD) was obtained by dividing the density of each band by the beta-actin density.

## Evaluation of irradiation treatments

Exponentially growing cells were seeded 1 day before irradiation and distributed into the following groups: (1) $^{10}$BPA + neutrons: cells were incubated with $^{10}$BPA at a dose of 10 µg $^{10}$B ml$^{-1}$ (192 µg ml$^{-1}$) during 16 h before irradiation; (2) $^{10}$BOPP + neutrons: cells were incubated with $^{10}$BOPP at a dose of 10 µg $^{10}$B ml$^{-1}$ (33 µg ml$^{-1}$) during 16 h before irradiation; (3) neutron beam (N): cells were irradiated with the neutron beam. A control group without irradiation for each treatment was added: Control (C), C $^{10}$BPA and C $^{10}$BOPP.

Each group of them was incubated with and without 1 mM NaB during 24 h before irradiation.

## Dosimetry

Cells were irradiated at the thermal column of the RA-3 reactor (Miller et al. 2009). This is an 8 MW reactor, located in Ezeiza, Argentina, where a highly thermalized and homogenous irradiation field is available. Thermal flux is near $(1.0 \pm 0.1) \times 10^{10}$ n cm$^{-2}$ s$^{-1}$, the cadmium ratio is 4,100 for gold foils, which allows neglecting fast neutron dose, and the gamma dose rate is approximately $(6.0 \pm 0.2)$ Gy h$^{-1}$.

Total dose is obtained by adding partial doses coming from photons, nitrogen capture (a 3.5 % wt of nitrogen content is assumed) and boron capture. Before each irradiation, neutron flux at the irradiation position is checked again using a calibrated Rh-SPND at the center of two T25 flasks or 96-well plates (with no cells inside) reproducing the configuration that is then used to irradiate the cells while, simultaneously, signal from a boron-coated ionization chamber is used as a monitor. Based on this measurement, irradiation times are calculated in order to deliver doses ranging from 1 to 5 Gy with an estimated uncertainty of 10 %.

Tables 1 and 2 show for each treatment, the time, the flux and each dose component of the total physical absorbed dose of the neutron beam without and with boron, respectively. As there is no reliable method to measure the boron intracellular concentration at the time of irradiation in vitro, we assumed that $^{10}$BPA and $^{10}$BOPP were uniformly distributed inside and outside the cells for the dosimetric calculations.

**Table 1** Dosimetry for thermal neutron irradiation without boron

| Irradiation time (s) | Thermal neutron flux (n $cm^{-2}$ $s^{-1}$) | Fluence (n $cm^{-2}$) | Dose γ (Gy) | Dose $^{14}N$ (Gy) | Total dose (Gy) |
|---|---|---|---|---|---|
| 1,001 | $(1.0 \pm 0.1) \times 10^{10}$ | $(9.5 \pm 0.8) \times 10^{12}$ | $2.33 \pm 0.04$ | $2.6 \pm 0.2$ | $5.0 \pm 0.2$ |
| 605 | $(1.0 \pm 0.1) \times 10^{10}$ | $(5.7 \pm 0.5) \times 10^{12}$ | $1.41 \pm 0.03$ | $1.6 \pm 0.1$ | $3.0 \pm 0.1$ |
| 202 | $(1.0 \pm 0.1) \times 10^{10}$ | $(1.9 \pm 0.2) \times 10^{12}$ | $0.470 \pm 0.009$ | $0.53 \pm 0.04$ | $1.00 \pm 0.04$ |

**Table 2** Dosimetry for thermal neutron irradiation with boron (neutrons plus 10 ppm $^{10}B$)

| Irradiation time (s) | Thermal neutron flux (n $cm^{-2}$ $min^{-1}$) | Fluence (n $cm^{-2}$) | Dose γ (Gy) | Dose $^{14}N$ (Gy) | Dose $^{10}B$ (Gy) | Total dose (Gy) |
|---|---|---|---|---|---|---|
| 381 | $(1.0 \pm 0.1) \times 10^{10}$ | $(3.6 \pm 0.3) \times 10^{12}$ | $0.89 \pm 0.02$ | $1.00 \pm 0.08$ | $3.1 \pm 0.4$ | $5.0 \pm 0.4$ |
| 228 | $(1.0 \pm 0.1) \times 10^{10}$ | $(2.2 \pm 0.2) \times 10^{12}$ | $0.53 \pm 0.01$ | $0.60 \pm 0.05$ | $1.9 \pm 0.2$ | $3.0 \pm 0.2$ |
| 76 | $(1.0 \pm 0.1) \times 10^{10}$ | $(7.2. \pm 0.6) \times 10^{12}$ | $0.177 \pm 0.005$ | $0.20 \pm 0.02$ | $0.60 \pm 0.08$ | $1.00 \pm 0.08$ |

### Cell surviving assay

For cell viability evaluation, 1,000 cells were seeded in 96-well plates. Eight different wells were seeded per treatment. After irradiation, the medium was changed and the cells were cultured at 37 °C. The medium was changed again at day 4 after irradiation and 20 µl of MTT 0.5 % w/v in PBS was added. The survival curves were fitted using the programme Origin 7.5 (OriginLab, USA) according to the linear-quadratic model (surviving fraction = $\exp^{-\alpha(D)-\beta(D)2}$). For each survival curve, the survival fraction was calculated at 2 Gy (SF2) after fitting the data. Each point in the curve is the result of three independent experiments.

### Frequency of cell death analysis

Cell death was evaluated morphologically by fluorescence microscopy (Olympus BX51, 40X) at 24- and 48-h post-irradiation. Briefly, cell pellets ($10^6$) were resuspended in 100 µl of a staining solution containing propidium iodide (PI), 4,5-diaminofluorescein (DAF) and Hoechst 33258 at the concentration of 0.6, 0.1 and 0.6 mg $ml^{-1}$, respectively. Results are expressed as percentage of living cells, apoptotic cells or necrotic cells per 200 total cells.

### Cell cycle analysis

To determine the distribution of cells in G1, S and G2/M cell cycle phases, proliferating cells were irradiated with 3 Gy of total physical dose. After 24- or 48-h post-irradiation, $10^6$ cells were washed three times with ice-cold PBS, fixed in absolute ethanol and stored at −20 °C, O/N. Cell pellets were resuspended in a staining solution of PBS containing 60 µg $ml^{-1}$ PI and 50 µg $ml^{-1}$ RNAase. The flow analysis was carried out using a flow cytometer (BD FACSCalibur). Processing and analysis of flow cytometry data were performed using Cylchred (Cardiff University) and WinMDI (created by Joe Trotter) softwares.

### Biodistribution studies

To evaluate the influence of NaB on $^{10}BPA$ uptake, animals received a single IP injection of NaB 24 h prior to the $^{10}BPA$ administration (500 µl of a 50 mM NaB in PBS solution) (Westphal et al. 2000). $^{10}BPA$-fructose (0.14 M) was injected 24 h later at a dose of 350 mg $kg^{-1}$ bw. All the mice were killed 0.5, 1, 2 and 3 h later, and the boron measurements in tissues and blood were performed by inductively coupled plasma optical emission spectroscopy (ICP-OES) employing an axially viewed plasma using an Optima 3100 instrument (Perkin-Elmer, Norwalk, CT). Digestion of tissue samples, with masses ranging between 10 and 50 mg, was carried out for 2 h at 60 °C with 0.15 ml of a 1:1 mixture of concentrated nitric and sulfuric acids. Dilution to 1.0 ml was performed with 0.65 ml of a 5 % aqueous solution of Triton X-100 (v/v) and 0.2 ml of a solution containing 25 µg $ml^{-1}$ Sr and 0.5 µg $ml^{-1}$ *Y* as internal standards. Analytical and internal standard lines (in nm) were as follows: *B,* 249.677; Sr, 232.235; and *Y,* 371.029. Matrix-matched standard solutions containing the internal standard elements and boron between 0.05 and 1 µg $ml^{-1}$ were employed for daily calibration.

### Statistical analysis

All results are expressed as the average of three independent experiments ± SEM. For statistical analysis of cell proliferation, one-way ANOVA and Dunnett's test were performed. Differences between the SF2 were calculated

with two-tailed Student's *t*-test. Differences were considered significant when $p < 0.05$.

## Results

The results of the evaluation of sodium butyrate effect in cell viability can be observed in Fig. 1a and b. WRO and FRTL-5 cells were incubated with increasing concentrations of NaB for 24 and 48 h. After 24 h of incubation, we observed an inhibitory effect of the drug only for the higher dose (1.5 mM) in both cell lines. On the other hand, longer times of incubation showed an effect of the drug with all the used doses ($p < 0.001$) at 48 h in WRO cells, while no inhibitory effect was observed in FRTL-5 cells. We chose to use a dose lower than 1.5 mM and the shorter time of incubation for the next experiments.

In normal (FRTL-5) and tumoral cells of thyroid (WRO), there was an accumulation of acetylated H3 after 24 h of incubation with the inhibitor NaB ($p < 0.05$) (Fig. 2a, b) at a dose of 1 mM compared to cells treated with and without both boron compounds (CBPA, CBOPP and Control, respectively).

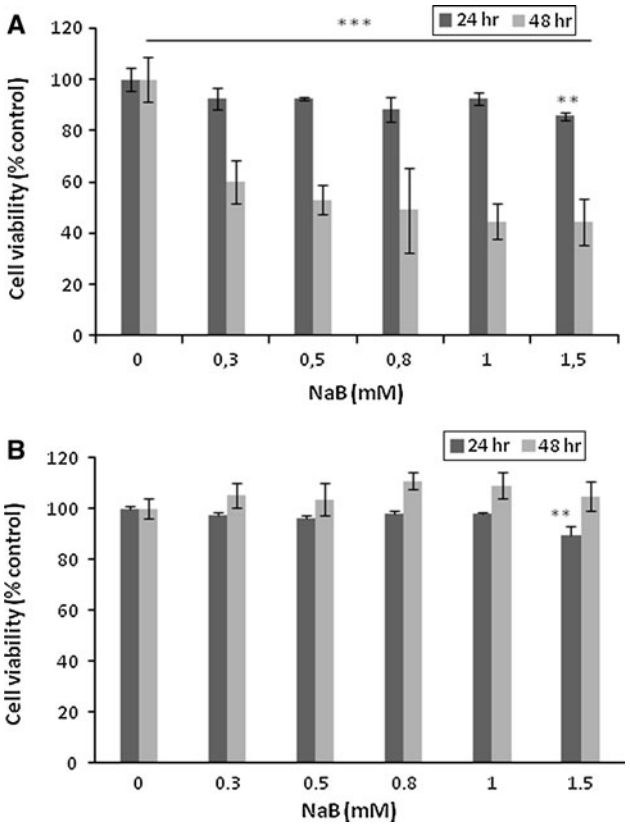


**Fig. 1** Effect of increasing doses of NaB on cell growth at 24 and 48 h in WRO tumor cell line (**a**) and FRTL-5 normal cell line (**b**). $^{**}p < 0.01$ NaB 1.5 mM versus Control at 24 h and $^{***}p < 0.001$ for all the used doses versus Control at 48 h

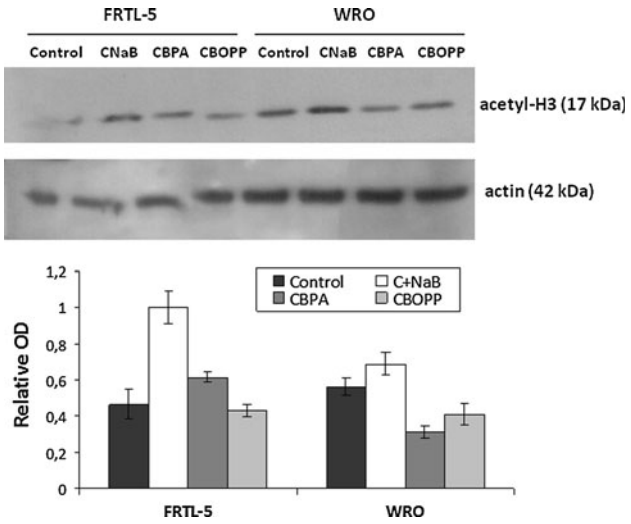


**Fig. 2** Histone 3 acetylation status measured after exposure to NaB. Cells were incubated with 1 mM NaB for 24 h and collected for Western blot analysis of acetylated histone 3. *Lane 1–4* corresponds to FRTL-5 cells: *Lane 1* Control, *Lane 2* Control + NaB (CNaB), *Lane 3* Control + BPA (CBPA) and *Lane 4* Control + BOPP (CBOPP). *Lane 5–8* corresponds to WRO cells: *Lane 5* Control, *Lane 6* Control + NaB (CNaB), *Lane 7* Control + BPA (CBPA) and *Lane 8* Control + BOPP (CBOPP). Histogram: Net intensity was calculated as the ratio between treated cells and untreated control. Data are the average of three independent experiments ± SEM. $^{*}p < 0.05$ C + NaB versus Control, CBPA and CBOPP

Figure 3 shows that there was a decrease in the surviving cell fraction in all irradiated groups in WRO cells incubated with NaB before irradiation (a, b and c). The effect of BNCT + NaB was higher than the effect produced by the irradiation with neutrons alone. In the N + $^{10}$BPA group, the SF2 decreased from 26.4 ± 1.3 to 19.5 ± 2.8 ($p < 0.05$) when adding NaB, while in the N + $^{10}$BOPP group, it decreases from 33.8 ± 2.9 to 20.1 ± 0.4 ($p < 0.01$) (Table 3a). On the contrary, the normal cell line (FRTL-5) showed to be more radioresistant and the pretreatment with NaB did not cause a significant decrease on cell survival fraction in the groups irradiated with neutrons alone and N + $^{10}$BPA (Fig. 4a, b; Table 3b). In the N + $^{10}$BOPP group, this effect was greater although not significant (Fig. 4c; Table 3b). These results agree with previous reports which demonstrated that NaB enhanced the radiosensitivity of different tumor cells, but not of the normal cells (Munshi et al. 2005; Cho et al. 2009).

At 24 and 48 h after an irradiation with 3 Gy, the effect of NaB on cell death levels was analyzed. At both times, there was an increase in apoptotic and necrotic cells in all irradiated groups compared to their respective control group. At 24 h, the addition of NaB increased significantly

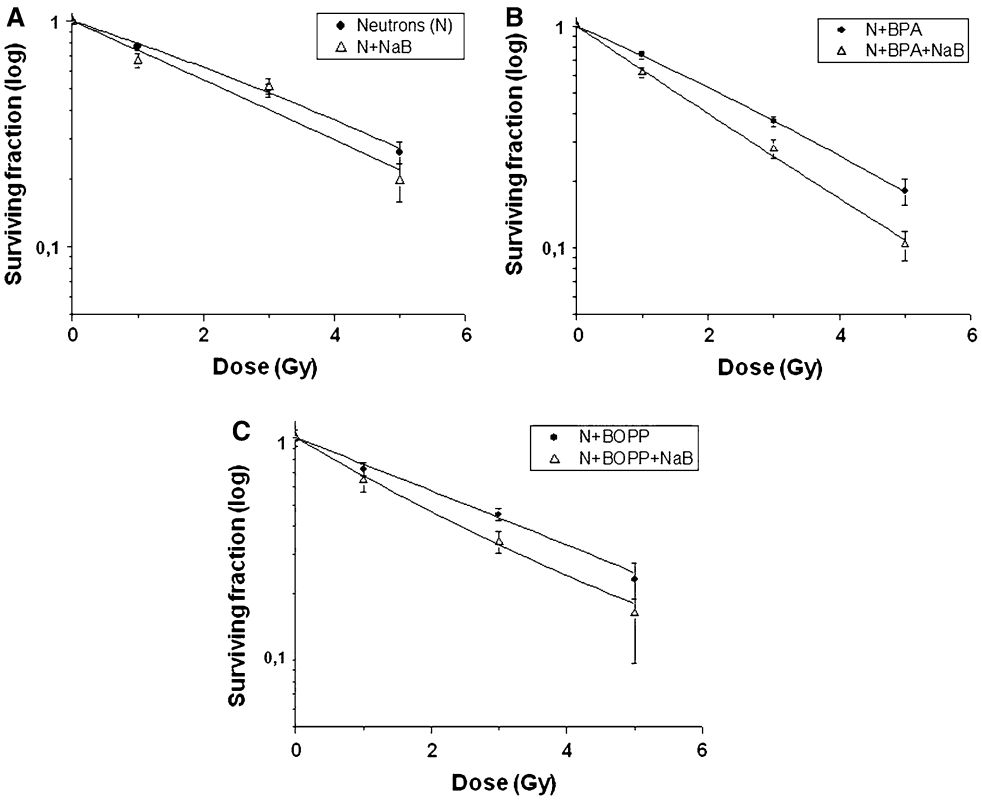


**Fig. 3** Effect of NaB on cell survival after irradiation. Cell survival curves of exponentially growing WRO cells incubated with or without NaB, irradiated with neutrons (N) (**a**), N + BPA (**b**) and N + BOPP (**c**). The *curves* were fitted according to the linear-quadratic model (surviving fraction = $\exp^{-\alpha(D)-\beta(D)2}$)

**Table 3** Survival fraction at 2 Gy (SF2) under different treatments

| Treatment | SF2 | |
|---|---|---|
| | Without NaB | With NaB |
| *A SF2 of WRO cells* | | |
| Neutrons (N) | 36.1 ± 6.1 | 27.5 ± 3.5 |
| BPA | 26.4 ± 1.3 | 19.5 ± 2.8* |
| BOPP | 33.8 ± 2.9 | 20.1 ± 0.4** |
| *B SF2 of FRTL-5 cells* | | |
| Neutrons (N) | 76.9 ± 7.4 | 77.6 ± 6.0 |
| BPA | 71.0 ± 3.0 | 66.0 ± 2.5 |
| BOPP | 62.9 ± 3.5 | 48.4 ± 6.4 |

SF2 values from each curve were calculated after fitting the survival curves with the quadratic lineal model (surviving fraction = $\exp^{-\alpha(D)-\beta(D)2}$) using the programme Origin 7.5 (OriginLab, USA). (a) SF2 of WRO cells. (b) SF2 of FRTL-5 cells

* $p < 0.05$ for N + BPA versus N + BPA + NaB

** $p < 0.01$ for N + BOPP versus N + BOPP + NaB

the percentage of apoptotic cells in the neutron beam ($p < 0.05$) and in the N + $^{10}$BPA ($p < 0.001$) groups. On the other hand, NaB increased the number of necrotic cells at 24 h in N ($p < 0.001$) and in N + $^{10}$BOPP groups ($p < 0.01$) (Fig. 5).

There was an increase in the percentage of cells which suffered a cell cycle arrest at G2/M phase in all irradiated groups compared to the control groups at both times studied (Table 4a, b). Addition of NaB increased the number of arrested cells in that phase of cell cycle in N + $^{10}$BPA group ($p < 0.05$) and in the N + $^{10}$BOPP group ($p < 0.001$). However, at 48-h post-irradiation, there were no differences in cells irradiated with or without NaB.

In this work as a first step toward the irradiation of the animals in the neutron beam, we also analyzed the effect of NaB on the biodistribution of $^{10}$BPA. The studies with animals showed a significant increase in the boron concentration in the tumor when NaB was administered 24 h before $^{10}$BPA injection (Table 5). The peak of boron in the tumor was 32.6 ± 1.4 (NaB) versus 22.54 ± 0.92 (Control) ppm at 2-h post-administration of $^{10}$BPA. The tumor/blood (T/B) ratios were 6.90 for $^{10}$BPA + NaB and 4.25 for $^{10}$BPA alone. In the case of the surrounding skin, the ratios were 2.90 and 2.12, respectively. The biodistribution of $^{10}$BPA in the other tissues did not show significant differences in the boron concentration when NaB was injected.

## Discussion

In the present studies, we investigated the possibility of enhancing the application of BNCT in the treatment of thyroid carcinoma using NaB as a radiosensitizer.

We have previously shown that BNCT can be an option to treat the undifferentiated and poorly differentiated

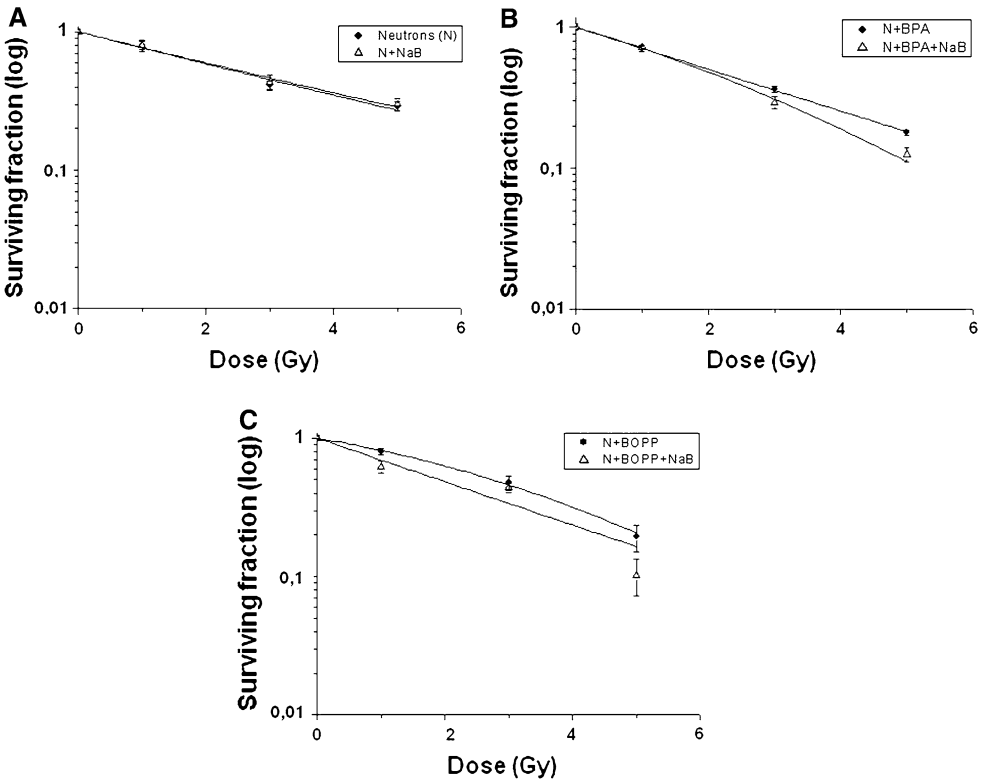


**Fig. 4** Effect of NaB on cell survival after irradiation. Cell survival curves of exponentially growing FRTL-5 cells incubated with or without NaB, irradiated with neutrons (N) (**a**), N + BPA (**b**) and N + BOPP (**c**). The *curves* were fitted according to the linear-quadratic model (surviving fraction = $\exp^{-\alpha(D)-\beta(D)2}$)

thyroid carcinoma (Pisarev et al. 2007). Thyroid carcinoma is usually treated with thyroidectomy followed by radioactive iodide administration. However, there are a number of patients with a high risk of local tumor recurrence due to microscopic residual disease. The recurrent tumor usually does not incorporate iodide making ineffective the conventional therapy (Brierley and Tsang 2008). Alternative treatments are necessary to offer an option to these patients.

We performed in vitro and in vivo studies using two different boron compounds: the aminoacid $^{10}$BPA and the porphyrin $^{10}$BOPP, alone and combined. In those studies, a complete remission during 3 months was achieved when tumors were smaller than 50 mm$^3$ and a 100 % halt of tumor growth when the tumor size was higher than 50 mm$^3$ for only 1 month (Koprinarova et al. 2010). Despite the promising experimental outcome of BNCT alone, the combination with treatments that improve the tumor response and decrease the radiation-induced damage to surrounding normal tissues would be desirable. In this regard, the combination with radiosensitizing compounds could be useful.

It has been previously demonstrated that sodium butyrate (NaB), a histone deacetylase inhibitor (HDACI), has an antitumoral effect by itself and in combination with other drugs used for chemotherapy (Dokmanovic et al. 2007). It was described that NaB can modulate nuclear proteins and DNA producing different effects like histone acetylation, phosphorylation, and hypermethylation of cytosine residues in DNA (Zhang et al. 2004). Therefore, HDACI have the propriety of modifying the DNA structure leaving the molecule opened and totally exposed to radiation. In this regard, there are studies performed in different tumoral cell lines or with in vivo models which were irradiated with gamma radiation (Camphausen et al. 2005; Marks et al. 2001).

In order to evaluate the possible use of the drug to enhance the radiation effects arising from BNCT, first we performed studies with NaB alone. We determined the dose and the incubation time with the drug without a significant effect on cell viability to perform the next experiments. Sodium butyrate decreased the viability of WRO tumor cells at 48 h after incubation at all the used doses, while no similar inhibitory effects were observed for FRTL-5 normal cells. It has been well documented that HDACI have growth-inhibitory effects by themselves in almost all transformed cell types, including cell lines derived from haematological and epithelial tumors (Arundel et al. 1985). On the contrary, in our studies at 24-h post-incubation, there was a cytotoxic effect only in cells incubated with the higher dose (1.5 mM) in both cell lines. We decided then to use a dose lower than 1.5 mM and the shorter time of incubation for the next experiments.

Pretreatment with NaB for 24 h before irradiation induced a significant decrease in the survival cell fraction in all the irradiated groups (N; N + $^{10}$BPA; N + $^{10}$BOPP) in WRO cells. This effect was higher in the groups incubated with boron compounds than in those without boron compounds

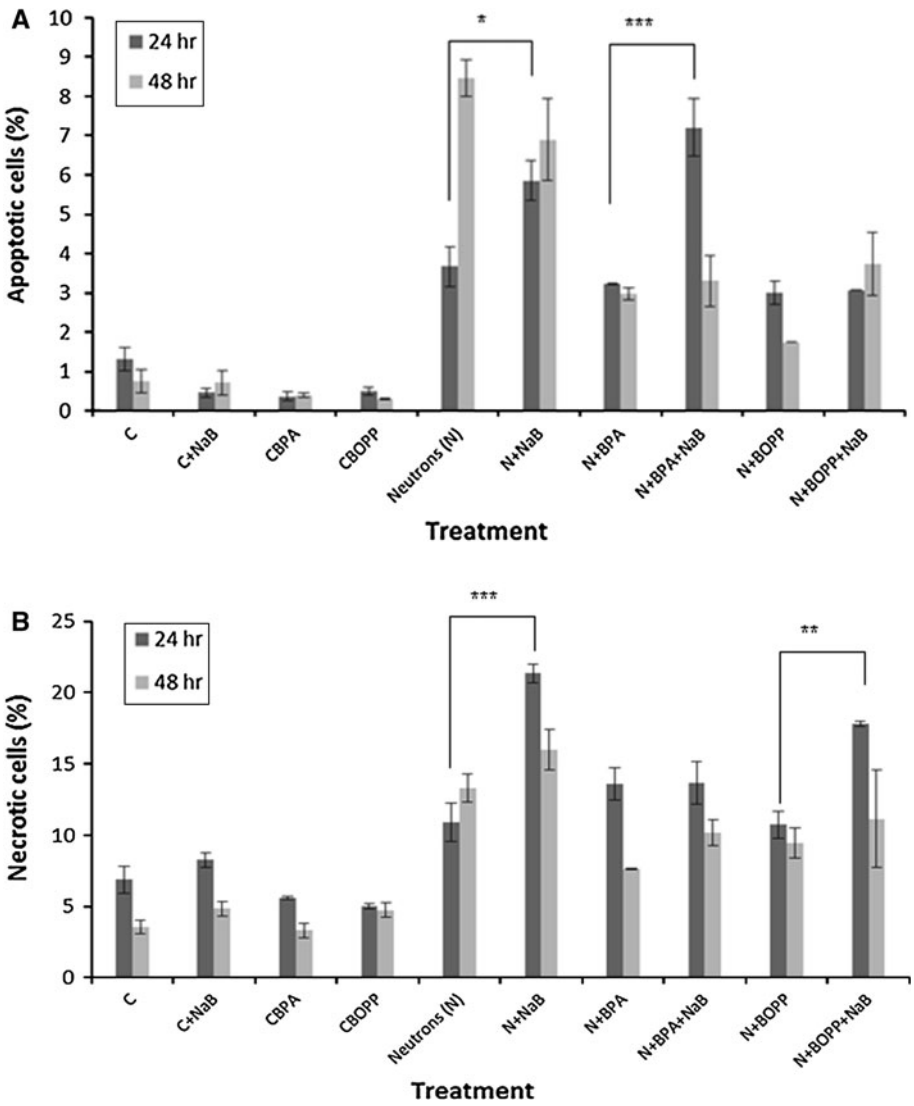


**Fig. 5** Frequency of cell death. Percentage of apoptotic cells **a** and necrotic cells **b** was evaluated 24- and 48-h post-irradiation. **a** $*p < 0.05$ for N versus N + NaB; $***p < 0.001$ for N + BPA versus N + BPA + NaB. **b** $**p < 0.01$ N versus N + NaB; $***p < 0.001$ for N + BOPP versus N + BOPP + NaB

and irradiated with the neutron beam. When the study was performed in normal thyroid cells, no radiosensitivity enhancement was observed in cells incubated with NaB. Another study performed with different cell lines showed a similar effect of the HDACI when cells were irradiated with gamma radiation (Ungerstedt et al. 2005). On the other hand, the incubation with NaB induced an accumulation of acetylated histone H3 in both cell lines. This fact could suggest that the radiosensitizing effect of NaB might be mediated by the accumulation of acetylated histones. The mechanism of the sensitivity of tumor cells and the relative resistance of normal cells to HDACI are still unclear. It has been demonstrated that the HDACI vorinostat caused cancer cell death at doses that cause little or no death of normal cells. Pilch et al. (2003) showed that the drug induced an accumulation of γH2AX, a marker of DNA double-strand breaks (DSBs) in both normal and transformed cells (Lee et al. 2010). It was also found that there was a suppression in the expression of DNA damage repair proteins in transformed but not in the normal cells treated with the HDACI (Pelicci and Minucci 2006).

The mechanisms of tumoral death, with and without sodium butyrate, were evaluated. We observed an increase in the apoptotic and necrotic cells in all the irradiated groups ($^{10}$BPA + N; $^{10}$BOPP + N; and N alone) compared to their corresponding control groups at 24- and 48-h post-irradiation. On the other hand, both types of death were higher in all the irradiated groups when the tumor thyroid cells were incubated with NaB. Treatment with HDACI has been found to alter the gene expression of proapoptotic and antiapoptotic genes. The induction of different cell death pathways through multiple mechanisms may be associated with the structural diversity of the HDACI (Ruefli et al. 2005). Furthermore, several studies have also demonstrated that the lethal effects of the HDACI could involve generation of reactive oxygen species (ROS) (Maggio et al. 2004) and ceramide (Richon et al. 2000).

**Table 4** Cell cycle analyses

| Cell cycle phase | Control | C + NaB | C BPA | C BOPP | *N* | N + NaB | N + BPA | N + BPA + NaB | N + BOPP | N + BOPP + NaB |
|---|---|---|---|---|---|---|---|---|---|---|
| *A 24-h post-irradiation* | | | | | | | | | | |
| G1 | 47.2 ± 10 | 50.2 ± 7.9 | 49.6 ± 0.8 | 51.7 ± 0.9 | 46 ± 3.9 | 40.4 ± 1.7 | 20.4 ± 6.9 | 14.51 ± 6.6 | 31.05 ± 4.3 | 17.2 ± 0.8 |
| S | 47.3 ± 8.9 | 37.6 ± 8.9 | 40.6 ± 1.6 | 40.4 ± 0.7 | 40 ± 5.6 | 35.1 ± 5.6 | 57 ± 9.7 | 51.5 ± 0.4 | 47.9 ± 12.4 | 40.6 ± 2.8 |
| G2/M | 5.5 ± 1.3 | 12.2 ± 0.6 | 9.8 ± 1.7 | 7.9 ± 1.6 | 14 ± 0.8 | 24.5 ± 3 | 22.6 ± 0.9$^{\#}$ | 34 ± 2.3* | 21.1 ± 1.5$^{\#\#}$ | 42.2 ± 4.3*** |
| *B 48-h post-irradiation* | | | | | | | | | | |
| G1 | 54 ± 7.3 | 50.9 ± 0.4 | 61.3 ± 3 | 63.5 ± 0.9 | 51.8 ± 1.9 | 45.3 ± 3.6 | 35.9 ± 4.1 | 32.8 ± 6.4 | 37.4 ± 4.9 | 42.3 ± 1.1 |
| S | 40.2 ± 8.2 | 39.3 ± 3.3 | 34.6 ± 5.1 | 27.3 ± 2.9 | 29.4 ± 1.5 | 36.1 ± 6.5 | 37.6 ± 3.1 | 45.6 ± 8.9 | 37.9 ± 3.5 | 39.3 ± 5.3 |
| G2/M | 5.81 ± 0.72 | 9.83 ± 0.68 | 4.08 ± 0.72 | 9.28 ± 0.72 | 18.83 ± 2.77$^{\#}$ | 18.53 ± 4.32 | 26.5 ± 2.8$^{\#\#\#}$ | 21.57 ± 4.64 | 24.64 ± 2.7$^{\#\#}$ | 18.46 ± 1.53 |

Cell distribution in cell cycle's phases was analyzed 24-h (a) and 48-h (b) post-irradiation. 3a: $^{\#}$ $p < 0.05$ for N + BPA versus C BPA; $^{\#\#\#}$ $p < 0.001$ for N + BOPP versus C BOPP; and * $p < 0.05$ for N + BPA + NaB versus N + BPA; *** $p < 0.001$ for N + BOPP + NaB versus N + BOPP. 3b: $^{\#}$ $p < 0.05$ for N versus Control; $^{\#\#\#}$ $p < 0.001$ for N + BPA versus C BPA; $^{\#\#}$ $p < 0.01$ for N + BOPP versus C BOPP

**Table 5** Boron concentration in the different tissues of NIH nude mice bearing PDTC

| Tissue | 0.5 h | | 1 h | | 2 h | | 3 h | |
|---|---|---|---|---|---|---|---|---|
| | BPA | BPA + NaB | BPA | BPA + NaB | BPA | BPA + NaB | BPA | BPA + NaB |
| Tumor | 18.9 ± 0.7 | 18.7 ± 0.9 | 22.7 ± 0.8 | 27.4 ± 1.0*** | 22.5 ± 0.9 | 32.6 ± 1.4*** | 18.5 ± 1.4 | 24.3 ± 0.9** |
| Blood | 10.5 ± 0.2 | 7.9 ± 0.9 | 6.2 ± 0.4 | 7.9 ± 0.5 | 5.3 ± 0.3 | 4.7 ± 0.6 | 3.2 ± 0.4 | 3.6 ± 0.4 |
| Surrounding skin | 11.7 ± 2.4 | 12.5 ± 1.2 | 12.8 ± 1.6 | 12.9 ± 0.7 | 10.6 ± 1.4 | 11.4 ± 0.5 | 10.1 ± 1.3 | 8.6 ± 0.6 |
| Distal skin | 11.3 ± 1.1 | 12.9 ± 0.3 | 13.4 ± 1.5 | 16.9 ± 1.4 | 9.4 ± 0.8 | 13.2 ± 1.5 | 7.1 ± 0.9 | 9.2 ± 1.3 |
| Liver | 11.6 ± 0.5 | 12.3 ± 1.3 | 9.7 ± 0.3 | 9.0 ± 0.2 | 6.1 ± 0.5 | 7.0 ± 0.5 | 5.9 ± 0.7 | 5.8 ± 0.4 |
| Spleen | 18.9 ± 2.0 | 19.8 ± 1.9 | 13.6 ± 0.5 | 12.8 ± 0.4 | 8.0 ± 0.4 | 8.5 ± 1.3 | 8.2 ± 1.1 | 7.8 ± 0.4 |
| Kidney | 41.3 ± 2.2 | 40.3 ± 3.0 | 31.0 ± 1.7 | 27.7 ± 0.7 | 14.9 ± 0.9 | 15.6 ± 1.6 | 13.1 ± 0.8 | 13.7 ± 1.1 |
| Lung | 14.1 ± 2.4 | 17.5 ± 3.5 | 10.4 ± 0.4 | 9.9 ± 0.3 | 7.7 ± 0.9 | 7.6 ± 0.7 | 6.7 ± 0.7 | 7.1 ± 0.7 |

The measurements were performed at different times after BPA injection at a dose of 350 mg/Kg bw. The NaB was administered 24 h before boron compound at a dose of 50 mM. The values are the average ± SEM between 5 and 8 samples of two different experiments

** $p < 0.01$; *** $p < 0.001$

It was described that HDACI cause cell cycle arrest in G1 and/or G2/M phase (Marks et al. 2001). In our studies, we found an arrest in the G2/M phase of the cell cycle at both incubation times studied in all irradiated groups. The radiosensitizer NaB increased the percentage of arrested cells in the same phase at 24-h post-irradiation. The mechanism by which HDACI induce cell cycle arrest was shown to include the induction of cell cycle genes like CDKN1A, which encodes for the production of $p21^{WAF1/CIP1}$ (Vrana et al. 1999; Qiu et al. 2000). HDACI can also transcriptionally repress cyclin D and cyclin A genes resulting in the loss of CDK2 and CDK4 kinase activity (Detta and Cruickshank 2009).

After the in vitro results, as the next step toward the application of BNCT using NaB as a radiosensitizer, we performed in vivo studies. In this regard, the effect of NaB in the BPA uptake was analyzed. These results demonstrated that the amount of boron increases significantly and specifically in the tumor. This fact could be due to the amount or activity of the L-system of amino-acid transporter (LAT) that imports $^{10}$BPA into the cell. A high level of LAT expression was reported in tumor cell lines (Puppin et al. 2005). In preliminary results performed in vitro, we observed an upregulation of the expression of three isoforms of LAT (LAT2, LAT3 and LAT4) compared with the control group (data not shown). Altered transcription of a number of genes in different tumor cells was observed with the addition of NaB to the culture medium (Munshi et al. 2005; Zhang et al. 2010).

We found that sodium butyrate might, therefore, be used to improve the application of BNCT in the treatment of thyroid cancer by two mechanisms. On the one hand, NaB would increase the amount of $^{10}$BPA in the tumor. On the other hand, it would act as an effective radiosensitizer of the boron neutron capture reaction. Future work is addressed to the irradiation of animals in the nuclear reactor.

**Acknowledgments** This work was supported by grants from the Balseiro Foundation, the National Scientific and Technical Research Council (CONICET) and the National Agency of Scientific and Technological Promotion (ANPCYT).

**Conflict of interest** The authors declare that there is no conflict of interest in this paper.

## References

Arundel CM, Glicksman AS, Leith JT (1985) Enhancement of radiation injury in human colon tumor cells by the maturational agent sodium butyrate (NaB). Radiat Res 104:443–448

Brierley JD, Tsang RW (2008) External beam radiation therapy for thyroid cancer. Endocrinol Metab Clin North Am 37:497–509

Butler LM, Webb Y, Agus DB, Higgins B, Tolentino TR, Kutko MC, LaQuaglia MP, Drobnjak M, Cordon-Cardo C, Scher HI, Breslow R, Richon VM, Rifkind RA, Marks PA (2001) Inhibition of transformed cell growth and induction of cellular differentiation by pyroxamide, an inhibitor of histone deacetylase. Clin Cancer Res 7:962–970

Camphausen K, Cerna D, Scott T, Sproull M, Burgan WE, Cerra MA, Fine H, Tofilon PJ (2005) Enhancement of in vitro and in vivo tumor cell radiosensitivity by valproic acid. Int J Cancer 114:380–386

Cho HJ, Kim SY, Kim KH, Kang WK, Kim JI, Oh ST, Kim JS, An CH (2009) The combination effect of sodium butyrate and 5-Aza-2′-deoxycytidine on radiosensitivity in RKO colorectal cancer and MCF-7 breast cancer cell lines. World J Surg Oncol 7:49. doi:10.1186/1477-7819-7-49

Dagrosa MA, Thomasz L, Longhino J, Perona M, Calzetta O, Blaumann H, Jimenez Rebagliati R, Cabrini R, Kahl S, Juvenal GJ, Pisarev M (2007) Optimization of boron neutron capture therapy for the treatment of undifferentiated thyroid cancer. Int J Radiat Oncology Biol Phys 69:1059–1066

Detta A, Cruickshank GS (2009) L-amino acid transporter-1 and boronophenylalanine-based boron neutron capture therapy of human brain tumors. Cancer Res 69:2126–2132

Dokmanovic M, Clarke K, Marks P (2007) Histone deacetylase inhibitors: overview and perspectives. Mol Cancer Res 5:981–989

Joensuu H, Kankaanranta L, Tenhunen M, Saarilahti K (2011) Boron neutron capture therapy (BNCT) as cancer treatment. Duodecim 127:1697–1703

Kageji T, Mizobuchi Y, Nagahiro S, Nakagawa Y, Kumada H (2011) Clinical results of boron neutron capture therapy (BNCT) for glioblastoma. Appl Radiat Isot 69:1823–1825

Kahl SB, Koo MS (1992) Synthesis and properties of tetrakiscarborane-carboxylate esters of 2, 4-*bis* (-dihydroxyethyl) deuteroporphyrin IX. In: Allen BJ, Moore DE, Harrington BV (eds) Progress in Neutron Capture Therapy for Cancer. New York Plenum Press, pp 223–226

Koprinarova M, Markovska P, Iliev I, Anachkova B, Russev G (2010) Sodium butyrate enhances the cytotoxic effect of cisplatin by abrogating the cisplatin imposed cell cycle arrest. BMC Mol Biol 11:49

Lee JH, Choy ML, Ngo L, Foster SS, Marks PA (2010) Histone deacetylase inhibitor induces DNA damage which normal but not transformed cells can repair. PNAS 107:14639–14644

Leith JT (1988) Effects of sodium butyrate and 3-aminobenzamide on survival of Chinese hamster HA-1 cells after X irradiation. Radiat Res 114:186–191

Maggio SC, Rosato RR, Kramer LB, Dai Y, Rahmani M, Paik DS, Czarnik AC, Payne SG, Spiegel S, Grant S (2004) The histone deacetylase inhibitor MS-275 interacts synergistically with fludarabine to induce apoptosis in human leukemia cells. Cancer Res 64:2590–2600

Marks P, Rifkind RA, Richon VM, Breslow R, Miller T, Kelly WK (2001) Histone deacetylases and cancer: causes and therapies. Nat Rev Cancer 3:194–202

Miller ME, Quintana J, Ojeda J, Langan S, Thorp SI, Pozzi E, Sztejnberg ML, Estryk G, Nosal R, Saire E, Agrazar H, Graiño F (2009) New irradiation facility for biomedical applications at the RA-3 reactor thermal column treatments. Appl Radiat Isot 67:S226–S229

Muhlethaler-Mottet A, Meier R, Flahaut M, Bourloud KB, Nardou K, Joseph JM, Gross N (2008) Complex molecular mechanisms cooperate to mediate histone deacetylase inhibitors anti-tumor activity in neuroblastoma cells. BMC Mol Cancer 7:55

Munshi A, Kurland JF, Nishikawa T, Tanaka T, Hobbs ML, Tucker SL, Ismail S, Stevens C, Meyn RE (2005) Histone deacetylase

inhibitors radiosensitize human melanoma cells by suppressing DNA repair activity. Clin Cancer Res 11:4912–4922

Pelicci PG, Minucci S (2006) Histone deacetylase inhibitors and the promise of epigenetic (and more) treatments for cancer. Nat Rev Cancer 6:38–51

Pilch DR, Sedelnikova OA, Redon C, Celeste A, Nussenzweig A, Bonner WM (2003) Characteristics of gamma-H2AX foci at DNA double-strand breaks sites. Biochem Cell Biol 81:123–129

Pisarev MA, Dagrosa MA, Juvenal GJ (2007) Boron neutron capture therapy in cancer: past, present and future. Arq Bras Endocrinol Metabol 51:852–856

Puppin C, D'Aurizio F, D'Elia AV, Cesaratto L, Tell G, Russo D, Filetti S, Ferretti E, Tosi E, Mattei T, Pianta A, Pellizzari L, Damante G (2005) Effects of histone acetylation on sodium iodide symporter promoter and expression of thyroid-specific transcription factors. Endocrinology 146:3967–3974

Qiu L, Burgess A, Fairlie DP, Leonard H, Parsons PG, Gabrielli BG (2000) Histone deacetylase inhibitors trigger a G2 checkpoint in normal cells that is defective in tumor cells. Mol Biol Cell 11:2069–2083

Richon VM, Sandhoff TW, Rifkind RA, Marks PA (2000) Histone deacetylase inhibitor induces p21 expression and gene associated histone acetylation. Proc Natl Acad Sci USA 97:10013–10019

Ruefli AA, Ausserlechner MJ, Bernhard D, Sutton VR, Tainton KM, Kofler R, Smyth MJ, Johnstone RW (2005) The histone deacetylase inhibitor and chemotherapeutic agent suberoylanilide hydroxamic acid (SAHA) induces cell death pathway characterized by cleavage of Bid and production of reactive oxygen species. Proc Natl Acad Sci USA 98:10833–10838

Ungerstedt JS, Sowa Y, Xu WS, Shao Y, Dokmanovic M, Perez G, Ngo L, Holmgren A, Jiang X, Marks PA (2005) Role of thioredoxin in the response of normal and transformed cells to histone deacetylase inhibitors. Proc Natl Acad Sci USA 102:673–678

US Department of Health and Human Services (1985) Guide for the care and use of laboratories animals. Public Health Service, National Institute of Health NIH Publication 86–23

Vrana JA, Decker RH, Johnson CR, Wang Z, Jarvis WD, Richon VM, Ehinger M, Fisher PB, Grant S (1999) Induction of apoptosis in U937 human leukemia cells by suberoylanilide hydroxamic acid (SAHA) proceeds through pathways that are regulated by Bcl-2/Bcl-x (L), c-Jun, and p21 (CIP1), but independent of p53. Oncogene 18:7016–7025

Westphal EM, Blackstock W, Feng W, Israel B, Kenney SC (2000) Activation of lytic Epstein-Barr virus (EBV) infection by radiation and sodium butyrate in vitro and in vivo: a potential method for treating EBV-positive malignancies. Cancer Res 60:5781–5788

Xu WS, Parmigiani RB, Marks PA (2007) Histone deacetylase inhibitors: molecular mechanisms of action. Oncogene 26:5541–5552

Zhang Y, Jung M, Dritschilo A, Jung M (2004) Enhancement of radiation sensitivity of human squamous carcinoma cells by histone deacetylase inhibitors. Radiat Res 161:667–674

Zhang Y, Bao YL, Wu Y, Yu CL, Sun Y, Li YX (2010) Identification and characterization of the human SLC5A8 gene promoter. Cancer Genet Cytogenet 196:124–132